UNIVERSITY *of York*

This is a repository copy of *A theory of alternative methods for measurements of absorption cross section and antenna radiation efficiency using nested and contiguous reverberation chambers*.

White Rose Research Online URL for this paper:
https://eprints.whiterose.ac.uk/97408/

Version: Accepted Version

Article:

White Rose
university consortium
Universities of Leeds, Sheffield & York

eprints@whiterose.ac.uk
https://eprints.whiterose.ac.uk/

A Theory of Alternative Methods for Measurements of Absorption Cross Section and Antenna Radiation Efficiency Using Nested and Contiguous Reverberation Chambers

Angelo Gifuni[1], Ian D. Flintoft[2], Simon J. Bale[2], Gregory C .R Melia[3] and Andy C. Marvin[2]

[1] Dipartimento di Ingegneria, Università di Napoli Parthenope, Centro Direzionale di Napoli, Isola C4, 80143Napoli, Italy
[2]Department of Electronics, University of York, Heslington, York YO10 5DD, UK
[3]Department of Physics, University of York, Heslington, York YO10 5DD, UK

A Theory of Alternative Methods for Measurements of Absorption Cross Section and Antenna Radiation Efficiency Using Nested and Contiguous Reverberation Chambers

Angelo Gifuni, *Member, IEEE*, Ian D. Flintoft, *Senior Member, IEEE*, Simon J. Bale, *Member, IEEE*, Gregory C. R. Melia, *Member, IEEE* and Andy C. Marvin, *Fellow, IEEE*

Abstract—Average ACS can be measured in a reverberation chamber; however, the existing technique determines a value that includes the effects of the radiation efficiencies of the antennas used in the measurement. Correcting for these necessitates further complex measurements. Here we present the theory of an alternative measurement methodology using two nested or contiguous reverberation chambers which is free from errors caused by the radiation efficiencies of the antennas. The new method is based on the theoretical average transmission cross sections (TCSs) of circular holes in a metal plate between the two chambers. In fact the method can be viewed as an accurate transfer calibration measurement between TCS and ACS that is independent of both the chamber and antenna characteristics. Further, since the existing method of measuring ACS includes the effects of the radiation efficiencies of the antennas, a comparison of the ACS of a reference object, measured using both the existing and new methods, also provides an alternative method of determining radiation antenna efficiency. Measurement uncertainties for both alternative measurement methods – ACS and antenna radiation efficiency – are also derived.

Index Terms—reverberation chambers, absorption cross sections, antenna radiation efficiency.

Thoughts on Professor Paolo Corona
by Angelo Gifuni

Prof. Paolo Corona was a pioneer in reverberation chambers; he devoted his life to his work. At the University of Naples Parthenope he sought to create an international center of excellence for reverberation chamber and electromagnetic compatibility research. I was part of this effort as Prof. Corona was both my advising Professor and later my supervisor; during the last years we also became friends. I will very much miss our pleasant and insightful discussions.

Manuscript received 10th December, 2015; revised 11th Mach, 2016.
Angelo Gifuni is with the Dipartimento di Ingegneria, Università di Napoli Parthenope, Centro Direzionale di Napoli, Isola C4, 80143 Napoli, Italy. (email: angelo.gifuni @uniparthenope.it).
Ian D. Flintoft, Simon J. Bale and Andy C. Marvin are with the Department of Electronics, University of York, Heslington, York, YO10 5DD, U.K. (e-mail: ian.flintoft@york.ac.uk; simon.bale@york.ac.uk; andy.marvin@york.ac.uk).
Gregory C. R. Melia is with the Department of Physics, University of York, Heslington, York, YO10 5DD, U.K. (email: g.melia@york.ac.uk).

I. INTRODUCTION

A reverberation chamber (RC) is a large cavity in which the fields are usually randomized by the movement of large metallic paddles that produce a change of the boundary conditions [1]. A combination of stirring techniques can be used in order to make the stirring process more effective [2]-[3]. RC techniques have been applied to many new applications in recent years [4]. These include: radiated immunity and emission testing; shielding characterization of cables, connectors, and materials; measurement of absorption and heating properties of materials; investigation of biological and biomedical effects; testing wireless devices; simulating wireless multipath environments; antenna efficiency measurements; and others [5].

The measurement of absorption cross section (ACS) is an important RC application [2], [6]-[11]. When measured using the standard approach, the ACS includes errors due to the radiation efficiencies of the antennas [6]-[11]. The error component resulting from the mismatches of the antennas can be easily removed [2], [3], whereas it is not easy to remove the error component due to the radiation efficiencies of the antennas. Manufacturers of antennas seldom supply such information in the specifications; therefore, correcting for it implies the measurement of the radiation efficiency of the antennas. This can be done in an RC [12]-[13]; however, it requires a rather complex procedure. Normally, the measurements of ACS are not corrected for antenna radiation efficiencies. ACS can also be measured using a time-domain approach; however, in this case the free volume of the chamber has to be known accurately [5], [12].

The goal of this paper is to present the theory of an alternative method for measurement of ACS that is free from the error due to the efficiencies of the antennas. The method uses nested RCs (NRCs) or contiguous RCs (CRCs); it is based on the theoretical average transmission cross section (TCS) of circular holes in a perfectly conducting sheet [6], [14]. Analytical solutions are available for the TCS of a circular aperture [6], [14], and good, simple approximations are available for both electrically large and electrically small apertures [6]. Numerical simulations can also be made to determine accurate values of average TCS in the resonance

region, which also account for the thickness of the metal plate. Holes with different shapes can be used, as well as any other transmission system, as long as their average TCS can be accurately calculated.

This work takes as its starting point the possibility of relating the wall losses and the TCS of an aperture in a wall of an RC shown by the Prof. Paolo Corona, together with other Authors, in [1, App. II], [15, eqs. (1) and (2)]. Actually, the TCS of such circular holes can also be measured [16, eqs. (11)-(12)]; however, such a measurement includes the antenna radiation efficiencies and therefore cannot be used for our current purposes. Furthermore, by comparing the ACS of an object measured by both the current method and the one proposed here, an alternative method for measurement of antenna radiation efficiency is also achieved. In this case the ACS of the object to be measured can be chosen so as to optimize the relevant uncertainties.

Since the field in the RC is randomized, all relevant physical quantities in what follows are implicitly meant in the sense of an average over an ensemble of independent field configurations. For an ACS measurement made by the current method, in which we assume that only the mismatch efficiencies are accounted for, we can write:

$$\sigma_{meas} = \frac{1}{\eta_{rad,tx}\eta_{rad,rx}}\sigma_{tr}, \tag{1}$$

where σ_{meas} and σ_{tr} are the measured and true values of the ACS and $\eta_{rad,tx}$ and $\eta_{rad,rx}$ are the radiation efficiencies of the transmitting and receiving antenna, respectively. The absolute error E_a and the relative error E_r for an ACS measurement due to the radiation efficiencies are, respectively:

$$E_a = \sigma_{tr}\left(\frac{1-\eta_{rad,tx}\eta_{rad,rx}}{\eta_{rad,tx}\eta_{rad,rx}}\right), \tag{2}$$

$$E_r = \frac{1-\eta_{rad,tx}\eta_{rad,rx}}{\eta_{rad,tx}\eta_{rad,rx}}. \tag{3}$$

Note that the simplification is obvious for (1)-(3) when $\eta_{rad,tx} = \eta_{rad,rx} = \eta_{rad}$. As an example, we note that $E_r = 23.4\%$ when $\eta_{rad,tx} = \eta_{rad,rx} = \eta_{rad} = 0.9$. In Section II, we develop the measurement theory for ACS in the case of NRCs; then in Section III, the case of CRCs is shown. In Section IV, the measurement of antenna radiation efficiency is presented and we discuss the practical implementation of the methods in Section V; some results of preliminary tests for validations are also shown. Finally in Section VI, conclusions are drawn.

II. ACS MEASUREMENTS USING NRCS

We first consider a system of nested RCs as shown in Fig.1. The two receiving antennas, RX$_o$ and RX$_i$, which are placed in the outer and inner chambers, are assumed to be identical. The NRC system is fed by an antenna, TX$_o$, in the outer chamber. We can write [16], [17]:

$$SE_{ic} = \frac{\dfrac{P_{rx,o}}{P_{tx,o}}}{\dfrac{P_{rx,i}}{P_{tx,o}}} = \frac{IL_{o,c}}{IL_{o,ic}} = \frac{P_{rx,o}}{P_{rx,i}}, \tag{4}$$
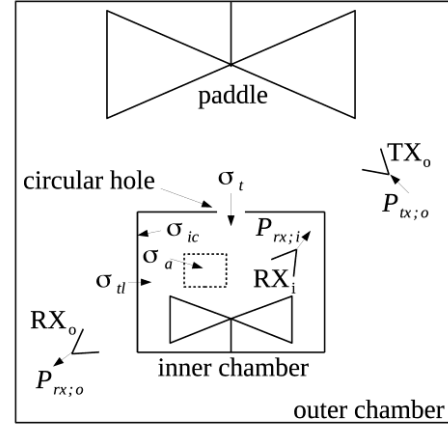

Fig. 1. Nested reverberation chambers.

where SE_{ic} is the shielding effectiveness (SE) of the inner chamber; $P_{rx,0}$ is the power received by a receiving antenna placed in the outer chamber; $P_{rx,i}$ is the power received by a receiving antenna placed in the inner chamber; $P_{tx,o}$ is here considered to be the incident power at the reference plane of the transmitting antenna. In practice, the ratios $P_{rx,0}/P_{tx,0} = IL_{o,c}$ and $P_{rx,i}/P_{tx,o} = IL_{o,ic}$ correspond to the mean square values of the transmission coefficients measured by a network analyzer. The subscript o, (i) is referred to the outer (inner) chamber parameters. $IL_{o,c}$ is the insertion loss (IL) of the outer chamber; $IL_{o,ic}$ is the IL obtained when the power is transmitted from the outer chamber and received by the inner one.

Note that the measurements of IL normally include the total efficiency of the antennas. In this paper, unless otherwise specified, the measurements of IL are considered to be uncorrected for the mismatches of the antennas. Note that some authors use a definition of IL such that its value in dB is negative [10], as is the case here. For ACS measurements made by the method proposed here, only three antennas are strictly necessary.

Note that the SE_{ic} measurement is free from errors due to the efficiencies of the antennas, both the radiation and total efficiencies. If the receiving antenna in the inner chamber is a monopole antenna, an identical monopole is used as a receiving antenna in the outer chamber. Here, the mismatches of the two monopoles are assumed to be equal so that (4) intrinsically corrects the relevant error.

When the inner chamber is unloaded and no circular aperture is present in its walls, we can write [17]:

$$SE_{ic,e} = \frac{\sigma_{tl} + \sigma_{ic}}{\sigma_{tl}}, \tag{5}$$

where $SE_{ic,e}$ is the shielding effectiveness of the inner chamber when it is not loaded (empty); σ_{tl} is the complete TCS of the walls of the inner chamber (leakage) and σ_{ic} is the total ACS inside the inner chamber. The latter includes the losses in the walls when the field impinges from inside of the inner chamber, the power received by the antenna in the inner chamber, and the losses in the possible objects in the inner chamber, which do not include the load whose ACS must be measured. When the inner chamber is loaded, (5) becomes:

$$SE_{ic,a} = \frac{\sigma_{tl} + \sigma_{ic} + \sigma_a}{\sigma_{tl}} = SE_{ic,e} + \frac{\sigma_a}{\sigma_{tl}}, \qquad (6)$$

where $SE_{ic,a}$ is the shielding effectiveness of the inner chamber when it is loaded by σ_a; σ_a is the ACS of the absorbing sample that must be measured. By manipulating (5) and (6), we can write:

$$\sigma_a = \left(SE_{ic,a} - SE_{ic,e} \right) \sigma_{tl}. \qquad (7)$$

Note that to determine σ_a, we need σ_{tl}. To this end, one or more circular holes can be made in the walls of the inner chamber in order to control the total TCS of the inner chamber. Circular holes are preferable for this purpose as analytical solutions are available [6], [14]. The TCS of the circular holes made in the walls of the inner chamber is denoted by σ_t. When σ_t is present, (5) and (7) become, respectively:

$$SE_{ic,e,h} = \frac{\sigma_{tl} + \sigma_t + \sigma_{ic}}{\sigma_{tl} + \sigma_t}, \qquad (8a)$$

$$\sigma_a = \left(SE_{ic,a,h} - SE_{ic,e,h} \right) \left(\sigma_t + \sigma_{tl} \right), \qquad (9a)$$

where $SE_{ic,a,h}$ corresponds to $SE_{ic,a}$ when one or more circular holes are present in the walls of the inner chamber.

If the inner chamber is fabricated carefully, then it is possible to achieve

$$\sigma_{tl} << \sigma_t. \qquad (10)$$

Therefore, σ_{tl} can be neglected. When (10) holds, then (8a) and (9a) become, respectively:

$$SE_{ic,e,h} = 1 + \frac{\sigma_{ic}}{\sigma_t}, \qquad (8b)$$

$$\sigma_a = \left(SE_{ic,a,h} - SE_{ic,e,h} \right) \sigma_t. \qquad (9b)$$

Note that (10) allows us the simplification of the model (9a). However, σ_{tl} can be experimentally determined; by manipulating (5) and (9a), we can write:

$$\sigma_{tl} = \frac{SE_{ic,e,h} - 1}{SE_{ic,e} - SE_{ic,e,h}} \sigma_t. \qquad (11)$$

Normally, the leakage for a fixture is not very repeatable; therefore, (10) is the preferred way to overcome this drawback.

The performance of the model (9b) improves in terms of measurement sensitivity, dynamic range, and relative uncertainty when

$$\sigma_t << \sigma_{ic}. \qquad (12)$$

In fact, under condition (12), the sensitivity of (9) increases, as well as its measurement dynamic range, as σ_a is determined by comparing it with σ_{ic} and not to $\sigma_{ic} + \sigma_t$. The dynamic range of the ACS measurement is therefore increased by using smaller values of TCS. The smaller σ_{ic} is, the smaller the noise level of the measurement is. Since σ_{ic} cannot be reduced beyond a certain limit, for small ACS values, small chambers should be used. By considering (10) and (12), we can write:

$$\frac{SE_{ic,a,h}}{SE_{ic,e,h}} = 1 + \frac{\sigma_a}{\sigma_{tl} + \sigma_t + \sigma_{ic}} \cong 1 + \frac{\sigma_a}{\sigma_{ic}}. \qquad (13)$$

By considering (5), (8a), and (9a), the conditions expressed by (10) and (12) can be respectively considered satisfied when
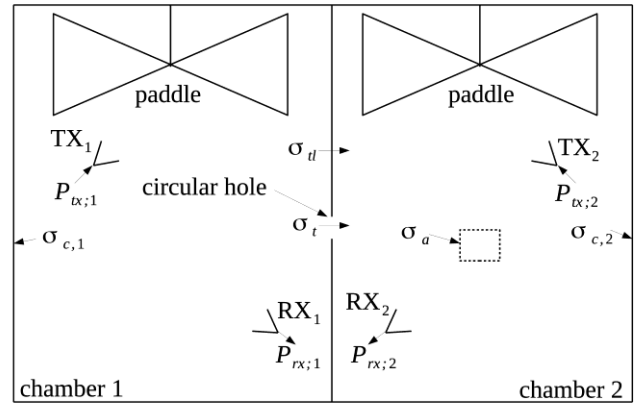

Fig. 2. Contiguous reverberation chambers.

$$\frac{SE_{ic,e}}{SE_{ic,e,h}} \geq 16 \text{ dB}, \qquad (14)$$

$$SE_{ic,e,h} \geq 5 \text{ dB}. \qquad (15)$$

Practically, 16 dB is an acceptable value in (14) to satisfy the condition (10). In fact, 16 dB in (14) implies an error between 2.5% and 5% according to the values of σ_{tl}, σ_t, and σ_{ic} in (9b); clearly, values greater than 16 dB imply less error. As an example, 20 dB in (14) implies an error between 1% and 2%. Similarly, 5 dB in (15) implies that (13) becomes $(SE_{ic,a,h}/SE_{ic,e,h}) = 1 + 0.75(\sigma_a/\sigma_{ic})$, which is an acceptable approximation; clearly, values greater than 5 dB imply a better approximation of (13). We note that $SE_{ic,e} \geq 21$ dB and $SE_{ic,e,h} \geq 5$ dB can be experimentally achieved (see Section V).

We stress that (14) and (15) express the conditions (10) and (12), respectively. Even if (15) is not an essential condition as it improves the performance only, here, we assume that it is satisfied in order to avoid the degradation of the uncertainty of the measurements, as it will be made clear below. In the experimental procedure, the holes can be covered by pieces of adhesive aluminum when $SE_{ic,e}$ is measured, or they can be electromagnetically closed in a different way. Note that the holes can be made in different walls of the inner chamber in order to avoid mutual couplings among the holes and to reduce the uncertainty due to the configuration of the system [18].

It is also noted that the measurements of all the necessary ILs can easily be made by a four port vector network analyzer (VNA), both for ACS measurements made by NRCs and by CRCs. When a port of the VNA is not used, it must be terminated by a matched load. The case where CRCs are used is considered below.

III. ACS MEASUREMENTS USING CRCs

The model developed in the previous section is perfectly valid for a system formed by two contiguous chambers [16]; Fig. 2 shows such a system, where the transmitting and receiving antennas are denoted by TX and RX, respectively. Actually, the common wall can be soldered all along the perimeter, so that the TCS is given only by the circular hole(s) made in the wall itself; in Fig. 2, one hole is considered. When more than one aperture is used, they must be

electromagnetically far apart in order to avoid mutual coupling. Note that leakage σ_{ll} due to junctions, access doors or windows is included as ACSs in $\sigma_{c,1}$ and $\sigma_{c,2}$, which correspond to σ_{ic} for chamber 1 and 2, respectively; any spurious coupling between the chambers is assumed to be absolutely negligible. Fig. 2 shows a system where the two chambers are the same size; however, this is not a necessary condition.

Note that for the application of (9b), only three antennas are necessary – the transmitting antenna in the chamber corresponding to the inner chamber is not necessary. Four identical antennas are shown in Fig. 2 because the measurement of σ_a by the use of a single chamber, which includes the antenna efficiency, allows us to develop an alternative method for the measurement of antenna efficiency, as shown in the next section. However, it is stressed that for ACS measurements free from the error due to the efficiencies of the antennas, only the two receiving antennas need to be identical.

For a CRC system, by assuming that chamber 2 corresponds to the inner chamber and by considering that σ_{ll} is absolutely negligible in this case, (9) becomes:

$$\sigma_a = SE_{c2,a} - SE_{c2,e} \quad \sigma_t = \left(\frac{IL_{c1,a}}{IL_{c1,2,a}} - \frac{IL_{c1,e}}{IL_{c1,2,e}} \right) \sigma_t, \quad (16)$$

where (16) is written both in term of the SE of chamber 2 and in terms of ILs. In particular, $SE_{c2,e}$ and $SE_{c2,a}$ are the SEs of chamber 2, when it is unloaded and loaded, respectively; $IL_{c1,e}$, and $IL_{c1,a}$ are the ILs of chamber 1, when it is unloaded and loaded, respectively; $IL_{c1,2,e}$, and $IL_{c1,2,a}$ are the ILs achieved by feeding the system from chamber 1 (corresponding to the outer chamber) and by receiving in chamber 2, when it is unloaded and loaded, respectively. We emphasize that the shielding effectivenesses in (16), i.e., $SE_{c2,e}$ and $SE_{c2,a}$, mean the electromagnetic separations between the two chambers.

Note that for a single small aperture, $IL_{c1,2,e}$ and $IL_{c1,2,a}$, are both *de facto* given by the product of two independent ILs [19], which represent two independent random variables. Therefore, by assuming the well-known distribution for each IL, the mean and variance of $IL_{c1,2,e}$ and $IL_{c1,2,a}$ can be determined [20], as well as their distribution [19], [21-23]. However, a few small apertures are sufficient to make $IL_{c1,2,e}$ and $IL_{c1,2,a}$ exponentially distributed [19]. In the following, it is assumed that a large aperture (or at least a few circular holes) is (are) present in the walls of chamber 2. The case of a single small circular aperture should be avoided as in this case the uncertainty of the measurements increases, as is made clear below. However, even if the derivation for a single small aperture are not detailed here, they have also been made; therefore, the results regarding this specific case will also be specified for completeness of the theory.

The uncertainty of (16), or equivalently (9b), can be estimated by estimating the uncertainty of the single ratios in the brackets. The well-known distributions for the ILs are assumed [18], [24-25]. By setting $IL_{c1,a} = X$, $IL_{c1,2,a} = Y$, $IL_{c1,e} = V$, $IL_{c1,2,e} = Z$, and $L = (X/Y) + (V/Z)$, we can write [20]:

$$\mu_{X/Y} = \frac{IL_{c1,a,0}}{IL_{c1,2,a,0}} \left(1 + \frac{1}{N} \right) \cong \frac{IL_{c1,a,0}}{IL_{c1,2,a,0}}, \quad (17a)$$

$$s_{X/Y}^2 = \frac{2}{N} \left(\frac{IL_{c1,a,0}}{IL_{c1,2,a,0}} \right)^2, \quad (17b)$$

$$\mu_{V/Z} = \frac{IL_{c1,e,0}}{IL_{c1,2,e,0}} \left(1 + \frac{1}{N} \right) \cong \frac{IL_{c1,e,0}}{IL_{c1,2,e,0}}, \quad (17c)$$

$$s_{V/Z}^2 = \frac{2}{N} \left(\frac{IL_{c1,e,0}}{IL_{c1,2,e,0}} \right)^2, \quad (17d)$$

$$\mu_L = \mu_{X/Y} - \mu_{V/Z} = \frac{IL_{c1,a,0}}{IL_{c1,2,a,0}} - \frac{IL_{c1,e,0}}{IL_{c1,2,e,0}}, \quad (18)$$

$$s_L^2 = \sigma_{X/Y}^2 + \sigma_{V/Z}^2 = \frac{2}{N} \left[\left(\frac{IL_{c1,a,0}}{IL_{c1,2,a,0}} \right)^2 + \left(\frac{IL_{c1,e,0}}{IL_{c1,2,e,0}} \right)^2 \right], \quad (19)$$

where N is the number of independent samples; $\mu_{X/Y}$, $\mu_{V/Z}$, and μ_L are the means of the relevant random variables (RVs) X/Y, V/Z, and L; $s_{X/Y}^2$, $s_{V/Z}^2$, s_L^2 are the variances of the relevant RVs. The standard deviations are here denoted by s in order to avoid confusion with the symbol of the ACSs. The subscript suffix ",0" denotes the mean of the relevant quantity. Using (18) and (19), we can write:

$$cv_L = cv_{\sigma_a} = \frac{\sigma_L}{\mu_L} = \sqrt{\frac{2}{N}} \frac{\sqrt{SE_r^2 + 1}}{SE_r - 1}, \quad (20)$$

where cv_L is the relative standard uncertainty (variation coefficient) of L and σ_a; SE_r is the ratio $SE_{c2,a,0}/SE_{c2,e,0}$; $SE_{c2,e,0}$ and $SE_{c2,a,0}$ are the mean values of SE of chamber 2 when it is unloaded and loaded, respectively.

By the current method, the ACS is measured by using a single chamber [6]-[11]. Therefore, if the power is transmitted and received in chamber 2 (which corresponds to the inner chamber), we can write [6]-[11]:

$$\sigma_{a,2} = \left(\frac{1}{IL_{c2,a}} - \frac{1}{IL_{c2,e}} \right) \frac{\lambda^2}{8\pi} = \frac{IL_{c2,e} - IL_{c2,a}}{IL_{c2,a} IL_{c2,e}} \frac{\lambda^2}{8\pi}, \quad (21)$$

where $\sigma_{a,2}$ is the value of the ACS σ_a, which is achieved when it is measured by using (21). The ILs in (21) should be corrected for possible mismatches of the antennas. Even when the two chambers are the same size, it is opportune to make the two measurements of σ_a in the same chamber.

Note that the comparison of (16), or equivalently (9b), and (21) implicitly makes clear the physical insight of (16). The difference between the electromagnetic separations of the two chambers, with load and with no load, connects directly σ_a and σ_t in (16), whereas the difference between the two ILs of a single RC (by considering them greater than one), with load and with no load, connects directly σ_a and the effective area of the receiving antenna, which is given by $\lambda^2/8\pi$, in (21). In other words, the electromagnetic separation depends on the ACS by σ_t whereas the IL depends on the ACS by $\lambda^2/8\pi$.

The uncertainty of $\sigma_{a,2}$ is addressed in [2], [18]. The relative standard uncertainty of $\sigma_{a,2}$ is repeated here for convenience; it can be put in the form [18, eq.13]:

$$cv_{\sigma_{a,2}} = \sqrt{\frac{1}{N}} \frac{\sqrt{IL_r^2 + 1}}{IL_r - 1}, \qquad (22)$$

where $IL_r = IL_{c2,e,0}/IL_{c2,a,0}$ [18] and $cv_{\sigma_{a,2}}$ is the relative standard uncertainty of $\sigma_{a,2}$. Note that (20) has the same form as (22). At first, as is so far the case in the literature [2]-[3], [5]-[13], the effects of the correction for impedance mismatches of the antennas are neglected [24]. However, such effects can really only be neglected when the antennas are sufficiently impedance-matched [24]; this issue is discussed in Section V.

Note that when (15) holds, IL_r and SE_r are essentially equal. In fact, we can write:

$$SE_r = \frac{SE_{c2,a,0}}{SE_{c2,e,0}} = 1 + \frac{\sigma_a}{\sigma_t + \sigma_{c2}} \cong 1 + \frac{\sigma_a}{\sigma_{c2}}. \qquad (23)$$

$$IL_r = \frac{IL_{c2,e,0}}{IL_{c2,a,0}} = \frac{\sigma_{c2} + \sigma_a}{\sigma_{c2}} = 1 + \frac{\sigma_a}{\sigma_{c2}}. \qquad (24)$$

By considering (21) and (22), the result in (20) is expected for (16). Equations (23) and (24) show that the two methods have essentially the same sensitivity under the assumed hypotheses. Using (20) and (22), we can write:

$$R_{cv} = \frac{cv_{\sigma_a}}{cv_{\sigma_{a,2}}} = \sqrt{2}. \qquad (25)$$

Note that by (16) or equivalently by (9), measurements free from the error due to the efficiencies of the antennas are achieved, but the relevant relative standard uncertainty is $\sqrt{2}$ times that of (21). Therefore, (16) gives the same relative standard uncertainty as (21) when the number of independent samples is doubled. If (15) were not satisfied, then (25) would include SE_r and IL_r according to (20) and (22), and the related relative uncertainty would deteriorate. We note that in the case of a single small aperture, the "2" in (17b), (17d), (19), (20), and (25) becomes a "3".

IV. RADIATION EFFICIENCY MEASUREMENTS OF ANTENNAS

When σ_a is measured as mentioned above and $\sigma_{a,2}$ is measured by using two antennas having the same radiation efficiency, then by the measurements of $\sigma_{a,2}$ and σ_a, which are independent, the radiation efficiency can be determined. In short, three antennas with the same radiation efficiency are necessary to determine the radiation efficiency.

In fact, by considering (1) and noting that the ILs in (21) are corrected for antenna mismatches, we find that:

$$\eta_{rad}^2 = q = \frac{\sigma_a}{\sigma_{a,2}}. \qquad (26)$$

If the ILs in (21) are not corrected for possible mismatches of the antennas, then (26) becomes:

$$\eta^2 = \frac{\sigma_a}{\sigma_{a,2,unc}}, \qquad (27)$$

where $\sigma_{a,2,unc}$ is the load ACS determined by (21) when the ILs are not corrected for possible mismatches of the antennas, and η is the total efficiency of the antennas.

The uncertainty of $\sigma_{a,2,unc}$ is found by using the uncorrected

ILs [18], [24]. In (26) $\eta_{rad}^2 = q$ has been defined for convenience: first we find the uncertainty of RV q and then that of η_{rad}. It is important to note that for the measurement of η_{rad} and η we can choose the ACS σ_a to be measured. We can choose both the value of σ_a and its distribution in the chamber, in the sense that σ_a can be formed from a sum of smaller ACSs from multiple objects that are properly distributed in the chamber. We can also realize σ_t as a sum of cross-sections from multiple small holes, properly separated from each other to reduce the error component due to the measurement system configuration [18]. By considering the optimal field conditions in an RC, good values of σ_a could be such that IL_r and SE_r, which are equal under the hypotheses made, turn out to be in the range of 2 to 6 [26].

To estimate the uncertainties of (26) and (27), the uncertainties of (16) and (21) are used. We can write [18]:

$$\mu_{\sigma_{a,2}} = \frac{\lambda^2}{8\pi} \frac{IL_{c2,e,0} - IL_{c2,a,0}}{IL_{c2,e,0} IL_{c2,a,0}} = \frac{\lambda^2}{8\pi} \frac{IL_r - 1}{IL_{c2,e,0}}, \qquad (28)$$

$$s_{\sigma_{a,2}}^2 = \frac{1}{N} \left(\frac{\lambda^2}{8\pi} \right)^2 \frac{IL_r^2 + 1}{IL_{c2,e,0}^2}, \qquad (29)$$

$$\mu_{\sigma_a} = \sigma_t \frac{IL_{c1,e,0}}{IL_{c1,2,e,0}} \left(SE_r - 1 \right), \qquad (30)$$

$$s_{\sigma_a}^2 = \sigma_t^2 \frac{2}{N} \left(\frac{IL_{c1,e,0}}{IL_{c1,2,e,0}} \right)^2 \left[SE_r^2 + 1 \right]. \qquad (31)$$

By using (28)-(31), after some algebra, we can write [20]:

$$\mu_q = \frac{\sigma_t}{\dfrac{\lambda^2}{8\pi}} \frac{\dfrac{IL_{c1,e,0}}{IL_{c1,2,e,0}}}{\dfrac{1}{IL_{c2,e,0}}} \left[1 + \frac{1}{N} \frac{IL_r^2 + 1}{IL_r - 1^2} \right] \cong \frac{\sigma_t}{\dfrac{\lambda^2}{8\pi}} \frac{\dfrac{IL_{c1,e,0}}{IL_{c1,2,e,0}}}{\dfrac{1}{IL_{c2,e,0}}} \qquad (32)$$

$$s_q^2 = \frac{1}{N} \frac{\sigma_t^2}{\left(\dfrac{\lambda^2}{8\pi} \right)^2} \frac{\left(\dfrac{IL_{c1,e,0}}{IL_{c1,2,e,0}} \right)^2}{\left(\dfrac{1}{IL_{c2,e,0}} \right)^2} \left\{ \frac{2 \left[SE_r^2 + 1 \right]}{SE_r - 1^2} + \frac{\left[IL_r^2 + 1 \right]}{IL_r - 1^2} \right\}, (33)$$

where the last step in (32) is justified as the term $IL_r^2 + 1 \left/ \left[IL_r^2 - 1 \; N \right] \right.$ is much less than one. Note that IL_r is considered to be equal to SE_r in (32) and (33), as mentioned above.

Now using (33), we can write:

$$s_q = \sqrt{\frac{1}{N}} \frac{\sigma_t}{\dfrac{\lambda^2}{8\pi}} \frac{\dfrac{IL_{c1,e,0}}{IL_{c1,2,e,0}}}{\dfrac{1}{IL_{c2,e,0}}} \sqrt{\left\{ \frac{2 \; SE_r^2 + 1}{SE_r - 1^2} + \frac{IL_r^2 + 1}{IL_r - 1^2} \right\}}. \qquad (34)$$

Note that if (15) were not satisfied, then (32) and (34) would be multiplied by the term $(SE_r - 1)/(IL_r - 1)$, whereas (33) would be multiplied by the term $((SE_r - 1)/(IL_r - 1))^2$. By manipulating (32) and (34), we have:

$$cv_q = \frac{s_q}{\mu_q} = \sqrt{\frac{1}{N}} \sqrt{\frac{2 \; SE_r^2 + 1}{SE_r - 1^2} + \frac{IL_r^2 + 1}{IL_r - 1^2}}. \qquad (35)$$

We specify that in case of a single small aperture, the "2" in (31), (33), (34), and (35) becomes a "3". If $IL_r = SE_r = 3$, we find that:

$$cv_q = \sqrt{\frac{1}{N}}\sqrt{\frac{20}{4}+\frac{10}{4}} = 2.73\sqrt{\frac{1}{N}}, \quad (36a)$$

whereas if $IL_r = SE_r = 4$:

$$cv_q = \sqrt{\frac{1}{N}}\sqrt{\left[\frac{51}{9}\right]} = 2.38\sqrt{\frac{1}{N}}. \quad (36b)$$

The mean and the variance of η_{rad} can be determined by an approximation process, as it is a function of the square root of q (that is to say, $\eta_{rad} = \sqrt{q}$) we can write [20]:

$$\mu_{\eta_{rad}} \cong \sqrt{\mu_q} - \frac{1}{8}s_q^2\ \mu_q^{-\frac{3}{2}}, \quad (37)$$

$$s_{\eta_{rad}}^2 \cong \frac{1}{2}s_q^2\ \frac{1}{\mu_q}. \quad (38)$$

By manipulating (36) and (37), we can write:

$$cv_{\eta_{rad}} = \frac{s_{rad}}{\mu_{rad}} = \frac{\sqrt{\frac{1}{2}}s_q}{\mu_q - \frac{1}{8}s_q^2\ \mu_q^{-1}} = \frac{\sqrt{\frac{1}{2}}cv_q}{1-\frac{1}{8}cv_q^2} \cong \sqrt{\frac{1}{2}}cv_q, \quad (39)$$

where the last step is justified as $cv_q \ll 1$. Note that the relative standard uncertainty of η_{rad} is slightly less than that of η_{rad}^2.

V. DISCUSSION AND PRELIMINARY TESTS

It is important to note that if N is acquired in such a way that the uncertainty component due to the measurement system configuration is neutralized [18], then (39) gives the relative standard uncertainty of η_{rad}. It can be reduced by increasing N, which can be achieved by using a combination of stirring techniques, such as the mode stirring, position stirring (or source stirring), and frequency stirring. In order to avoid the error due to the stress of the cables and connectors of the antennas, in our case, the source stirring can be approximately achieved by properly moving the absorbing sample in the useful volume of the chamber. As an example, we note that if $IL_r = SE_r = 4$ and $N = 10000$, then $cv_{\eta_{rad}} = 1.8\%$.

In the above developments, the effects of the correction for the impedance mismatches of the antennas have been neglected, as has so far been done in the literature [2]-[3], [5]-[13]. When such effects are considered, the variance and the variation coefficient (relative standard uncertainty) of each IL increase according to the mismatches of the antennas [24], as well as all the uncertainties presented here. However, this deterioration in uncertainty is common to all results present in the literature [2]-[3], [5]-[13]. Note that the quality-factor measurement of an RC includes an IL measurement, and when it is transformed into the time domain such an uncertainty propagates according to the mathematical process [12].

The conditions in (14) can be easily achieved up to 20 GHz for CRCs; they can be achieved for NRCs as well, even though in this case specific attention has to be paid to the reduction of the leakage. The conditions in (15) can also be easily achieved for CRCs from 1 GHz to 20 GHz using a large circular aperture by changing the volume of chamber 2. A large aperture is not sensitive to the frequency and it can work over a wide range of frequency. For NRCs, the conditions in (15) can still be satisfied by using a large circular aperture; however, the working frequency range is limited by the volume of the inner chamber [3]. The conditions in (15) could also be easily satisfied by using some small circular apertures; but, in this case the working frequency range is further limited as the TCS of a small aperture is strongly dependent on the frequency. If the resonant region is included, then the working frequency range can be widened. Moreover, in this case, the edge effects due to the thickness of the wall should be investigated.

If the total working frequency range is split into successive frequency sub-ranges, the volume of the inner chamber for NRCs, as well as those of chamber 2 in CRCs, can be limited when a large aperture is used. Hence, a large aperture working from the lower frequency of the working frequency range to the maximum frequency where (15) is still satisfied can be made in a wall of the chamber. It can then be covered by a metal plate including another large aperture working from the maximum frequency of the previous sub-range to the maximum frequency of the current sub-range, and so on, up to cover the total working frequency range. The subsequent metal plates can be accurately placed using aluminium tape to cover the original large aperture made in the wall of the chamber.

If instead of a large aperture, some small apertures are made, then the subsequent metal plates must be placed by a technique which minimizes the leakage as (14) must also be satisfied. The number of successive frequency sub-ranges required depends on the total working frequency range and on the volume of the inner chamber.

Some preliminary tests were made using nested chambers, with a single circular aperture of diameter 50 mm between them, from 5 GHz to 10 GHz. The outer chamber dimensions were 4.7 m × 3.0 m × 2.37 m and the inner chamber dimensions were 0.6 m × 0.7 m × 0.8 m. Three nominally identical bespoke monopole antennas with 60 mm diameter circular ground planes were fabricated for the measurements. The monopole lengths were 12.3 mm and vertical elements had dielectric (PTFE) sleeves of thickness 1.3 mm over 75 % of their lengths. A cube of radio absorbing material (RAM) with a side length of 76 mm was used to load the inner chamber. The RAM manufacturer's dielectric properties were used to estimate the cube's ACS using a Mie Series calculation for a sphere of the same surface area [27]. The measurements were made using a two-port VNA with a seven term unknown through calibration error model so that all the cables could remain unmoved between the calibrations and measurements between the different pairs of antennas required. The average TCS of the hole was determined using a series of high resolution full wave simulations with two orthogonal polarizations of incident plane-waves at twelve angles of incidence, averaged over 2π steradians using Gauss-
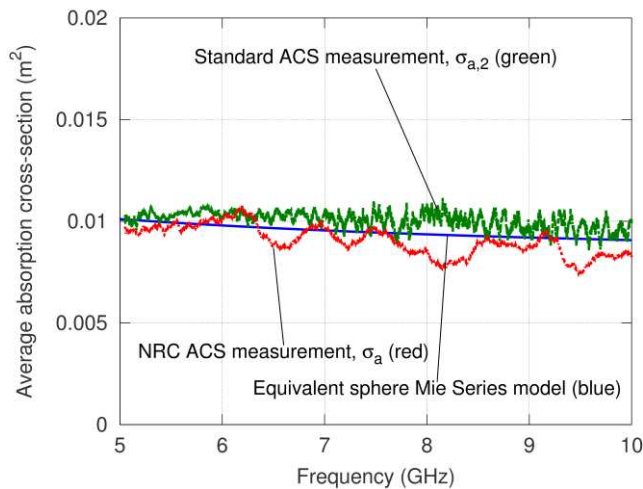
Fig. 3. Measured absorption cross-section of the RAM cube from a standard ACS measurement (including the correction for antennas mismatches) and the NRC ACS measurement compared to the Mie Series estimate.
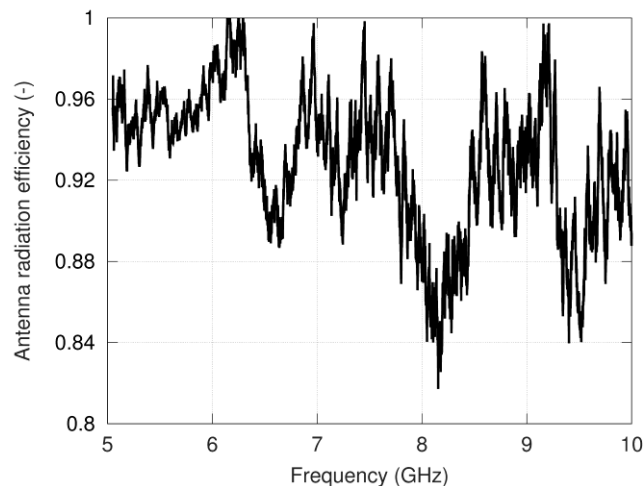

Fig. 4. Antenna radiation efficiency measured using the NRC approach, assuming that the monopole antennas are identical.

Legendre quadrature.

Fig. 3 shows the measured ACS of the RAM cube from a standard ACS measurement made in the small RC and from the proposed NRC measurement compared to the Mie Series estimate. The standard ACS measurement has been corrected for the free-space mismatch factors of the antennas but includes the effect of their radiation efficiencies. The NRC measurement, which does not include the effect of the radiation efficiencies of the antennas, is lower than the standard ACS measurement.

Taking the ratio of the two ACS measurements according to (26) we obtain the radiation efficiency of monopole antennas shown in Fig. 4. The radiation efficiency is mostly above 90 % and only makes a few very minor excursions above 100 % that are consistent with the predicted measurement uncertainty. This preliminary measurement did not utilize position (or platform) stirring so some systematic effects due to the non-ideal behavior of the chamber and direct coupling to the relatively large aperture may be present. Further work is continuing to determine the optimal measurement conditions for the NRC approach.

VI. CONCLUSIONS

An alternative method for measurement of ACS by nested or contiguous RCs has been presented. The method is based on the theoretical average TCS of circular holes in a perfectly conducting sheet. The ACS measurements by this method are free from errors due to the efficiencies of the antennas, whereas the ones made by the current method include the efficiencies of the antennas. In fact, the method can be used more generally as a transfer calibration measurement between TCS and ACS. The measurements can easily be made using a four-port network analyzer. A drawback of the method is the doubling of the number of independent samples needed to achieve the same uncertainty as the current method. However, this can be overcome by a combination of stirring techniques, such as mode stirring, position stirring (or source stirring) and frequency stirring. In order to avoid errors due to the stresses on the cables and connectors of the antennas, the source stirring can be approximately implemented by properly moving the absorbing sample in the stirred volume of the chamber.

Another drawback could be the reduced frequency agility, in the sense that the best conditions for the measurements are achieved for limited working frequency ranges. Therefore, measurements for a wide working frequency range may need to be achieved by concatenating results from several measurements, each taken with an aperture configuration appropriate to its frequency sub-range. Such a procedure can be automated. However, such drawbacks can be overcome by using chambers and apertures of appropriately large size.

By comparison of an ACS measurement of the same object made by the current method and the method proposed here, an alternative method for the measurement of the radiation efficiency of antennas has also been found. These measurements are taken with a known ACS value, which can be chosen, along with the distribution of absorbers in the chamber, so as to optimize the measurement conditions, and consequently the relevant measurement uncertainty, which has also been derived. Finally, some results of preliminary tests for validations are also shown.

REFERENCES

[1] P. Corona, G. Latmiral and E. Paolini, L. Piccioli, "Use of a reverberating enclosure for measurements of radiated power in the microwave range", *IEEE Trans. Electromagn. Compat.*, vol. 18, no. 2, pp. 54-59, May 1976.

[2] U. Carlberg, P.-S. Kildal, A. Wolfang, O. Sotoudeh and C. Orlenius, "Calculated and measured absorption cross sections of lossy objects in reverberation chamber", *IEEE Trans. Electromagn. Compat.*, vol. 46, no. 2, pp. 146-154, May 2004.

[3] C.L. Holloway, D. A. Hill, M. Sandroni, J. Ladbury, J. Coder, G. Koepke, A. C. Marvin and Y. He, "Use of reverberation chambers to determine the shielding effectiveness of physically small, electrically large enclosures and cavities", *IEEE Trans. Electromagn. Compat.*, vol. 50, no. 4, pp. 770-782, Nov. 2008.

[4] IEC 61000-4-21, *Electromagnetic Compatibility (EMC)*, Part 4-21: Testing and measurement techniques – Reverberation chamber test methods, International Electrotechnical Commission, Geneva, Switzerland, 2011.

[5] D.A. Hill, *Electromagnetic Fields in Cavities: Deterministic and Statistical Theories*, IEEE Press, New York, 2009.

[6] D.A. Hill, M.T. Ma, A.R. Ondrejka, B.F. Riddle, M.L. Crawford, R.T. Johnk, "Aperture excitation of electrically large, lossy cavities", *IEEE Trans. Electromagn. Compat.*, vol. 36, no. 3, pp. 169-177, Aug. 1994.

[7] P. Hallbjörner, U. Carlberg, K. Madsén and J. Anderson, "Extracting electrical material parameters of electrically large dielectric objects from reverberation chamber measurements of absorption cross section", *IEEE Trans. Electromagn. Compat.*, vol. 47, no. 2, pp. 291-303, May 2005.

[8] A. Gifuni, "On the measurement of the absorption cross section and material reflectivity in a reverberation chamber", *IEEE Trans. Electromagn. Compat.*, vol. 51, no. 4, pp. 1047-1050, Nov. 2009.

[9] G. Gradoni, D. Micheli, F. Moglie and V.M. Primiani, "Absorbing cross section in reverberation chamber: experimental and numerical results", *Prog. In Electromagn. Research B*, vol. 45, pp. 187–202, 2012.

[10] D. Senić, C.L. Holloway, J.M. Ladbury, G.H. Koepke and A. Šarolić, "Absorption characteristics and SAR of a lossy sphere inside a reverberation chamber", *2014 International Symposium on Electromagnetic Compatibility (EMC Europe)*, Gothenburg, Sweden, pp. 962-967, 1-4 Sept., 2014.

[11] I.D. Flintoft, G.C. R. Melia, M.P. Robinson, J.F. Dawson, and A.C. Marvin, "Rapid and accurate broadband absorption cross-section measurement of human bodies in a reverberation chamber", *IOP Measurement Science and Technology*, vol. 26, no. 6, art. no. 065701, pp. 1-9, May 2015.

[12] C.L. Holloway, H.A. Haider, R.J. Pirkl, W.F. Yong, D.A. Hill and J. Ladbury, "Reverberation chamber techniques for determining the radiation and total efficiency of antennas", *IEEE Trans. Electromagn. Compat.*, vol. 60, no. 4, pp. 1758-1770, Apr. 2012.

[13] X. Chen "Measurement uncertainty of antenna efficiency in a Reverberation Chamber", *IEEE Trans. Electromagn. Compat.*, vol. 55, no. 6, pp. 1331-1334, Dec. 2013.

[14] C.M. Butler, Y. Rahmat-Samii, and R. Mittra, "Electromagnetic penetration through apertures in conducting surfaces", *IEEE Trans. Antennas Propagat.*, vol. 26, no. 1, pp. 82-93, Jan. 1978.

[15] P. Corona, G. Latmiral, and E. Paolini, "Performance and analysis of a reverberating enclosure with variable geometry," *IEEE Trans. Electromagn. Compat.*, vol.22, pp. 2–5, Feb. 1980.

[16] A. Gifuni and M. Migliaccio, "Use of nested reverberating chambers to measure shielding effectiveness of nonreciprocal samples taking into account multiple interactions", *IEEE Trans. Electromagn. Compat.*, vol. 50, no. 4, pp. 783-786, Nov. 2008.

[17] A. Gifuni, "Relation between the shielding effectiveness of an electrically large enclosure and the wall material under uniform and isotropic field conditions", *IEEE Trans. Electromagn. Compat.*, vol. 55, no. 6, pp. 1354–1357, Dec. 2013.

[18] A. Gifuni, G. Ferrara, A. Sorrentino, and M. Migliaccio, "Analysis of the measurement uncertainty of the absorption cross section in a reverberation chamber", *IEEE Trans. Electromagn. Compat.*, vol. 57, no. 5, pp. 1262-1265, Oct. 2015.

[19] M. Höijer and L. Kroon, "Field statistics in nested reverberation chambers", *IEEE Trans. Electromagn. Compat.*, vol. 55, no. 6, pp. 1328-1330, Dec. 2013.

[20] D. Blumenfeld, *Operations Research Calculations Handbook*, CRC Press, New York, 2001.

[21] J. Salo, H. M. El-Sallabi and P. Vainikainen, "The distribution of the product of independent Rayleigh random variables", *IEEE Trans. Antennas Propag.*, vol. 54, no. 2, pp. 639-643, Feb. 2006.

[22] L. Kovalevsky, R. S. Langley, P. Besnier and J. Sol, "Experimental validation of the statistical energy analysis for coupled reverberant rooms", *2015 IEEE International Symposium on Electromagnetic Compatibility (EMC)*, Dresden, Germany, pp. 546 – 551, 16-22 Aug., 2015.

[23] G. Gradoni, T. M. Antonsen, S.M Anlage and E. Ott, "Random coupling model for interconnected wireless environments", *2014 IEEE International Symposium on Electromagnetic Compatibility (EMC)*, Raleigh, NC, pp. 792 – 797, 4-8 Aug., 2014.

[24] A. Gifuni, "Effects of the correction for impedance mismatch on the measurement uncertainty in a reverberation chamber", *IEEE Trans. Electromagn. Compat.*, vol. 57, no. 6, pp. 1724-1727, Dec. 2015.

[25] A. Gifuni, H. Khenouchi, and G. Schirinzi, "Performance of the reflectivity measurement in a reverberation chamber," *Prog. In Electromagn. Research PIER*, vol. 154, pp. 87–100, 2015.

[26] C.L. Holloway, D.A. Hill, J. M. Ladbury and G. Koepke, "Requirements for an effective reverberation chamber: Unloaded or loaded", *IEEE Trans. Electromagn. Compat.*, vol. 48, no. 1, pp. 187–193, Feb. 2006.

[27] I.D. Flintoft, S.J. Bale, S.L. Parker, A.C. Marvin, J.F. Dawson and M.P. Robinson, "On the measureable range of absorption cross-section in a reverberation chamber", *IEEE Transactions on Electromagnetic Compatibility*, vol. 58, no. 1, pp. 22-29, 2016.

Angelo Gifuni (M'10) received the Laurea degree in nautical science from the University of Naples "Parthenope," Napoli, Italy, in 1998. He is currently the Head of the Experimental Electromagnetism Laboratory, Department of Engineering, University of Naples "Parthenope".

His research interests include reverberation chamber, EMC and microwave measurements techniques, and shielding.

Ian D. Flintoft (M'00-SM'14) is a Research Fellow in the Physical Layer Research Group, University of York. He received B.Sc. and Ph.D. degrees in physics from the University of Manchester, Manchester, U.K., in 1988 and 1994, respectively.

His current research interests include electromagnetic compatibility (EMC), computational electromagnetics (CEM), electromagnetic exposure and bioelectromagnetics.

Simon J. Bale (S'05-M'12) obtained his MEng and PhD degrees in Electronics from the University of York, UK, in 2004 and 2012 respectively. He is currently a Research Fellow in same department.

His research interests include low noise microwave engineering, microelectronic design optimization and nano-scale analogue and digital design.

Gregory C. R. Melia (M'15) received MEng and PhD degrees in Electronic Engineering from the University of York, York, U.K. in 2008 and 2013 respectively. He is currently a Research Associate in the Department of Physics at the same institution.

His research interests include bioelectromagnetics and microwave engineering.

Andrew C. Marvin (M'85-SM'06-F'11) is Technical Director of York EMC Services Ltd and Professor of Applied Electromagnetics in the University of York's Department of Electronics. He received his BEng, MEng and PhD degrees from the University of Sheffield between 1972 and 1978.

His main research interests are EMC measurement and modelling techniques, EMC antennas and electromagnetic shielding measurement and modelling.